Analytical solution of susceptible-infected-recovered models on homogeneous networks

Louis Bremaud,[1] Olivier Giraud,[1,2,3] and Denis Ullmo[1]
[1]*Université Paris-Saclay, CNRS, LPTMS, 91405 Orsay, France*
[2]*MajuLab, CNRS-UCA-SU-NUS-NTU International Joint Research Laboratory, 117543 Singapore, Singapore*
[3]*Centre for Quantum Technologies, National University of Singapore, 117543 Singapore, Singapore*

(Received 15 December 2023; accepted 18 September 2024; published 17 October 2024)

The ability to actually implement epidemic models is a crucial stake for public institutions, as they may be overtaken by the increasing complexity of current models and sometimes tend to revert to less elaborate models such as the susceptible-infected-recovered (SIR) model. In our work, we study a simple epidemic propagation model, called SIR-k, which is based on a homogeneous network of degree k, where each individual has the same number k of neighbors. This model represents a refined version of the basic SIR which assumes a completely homogeneous population. We show that nevertheless, analytical expressions, simpler and richer than the ones existing for the SIR model, can be derived for this SIR-k model. In particular, we obtain an exact implicit analytical solution for any k, from which quantities such as the epidemic threshold or the total number of agents infected during the epidemic can be obtained. We furthermore obtain simple exact explicit solutions for small ks, and in the large k limit we find a new formulation of the analytical solution of the basic SIR model, which comes with new insights.

DOI: 10.1103/PhysRevE.110.044307

I. INTRODUCTION

Understanding the dynamics of epidemics is of primary importance to allow public policies to mitigate their negative impact [1,2]. Models of epidemic propagation have therefore been introduced as early as one century ago, in 1927, in particular, the seminal paper of Kermack and McKendrick [3]. In this paper, they introduce the susceptible-infected-recovered (SIR) model, which, despite its simplicity, is still a basis of work in many studies [4–6]. This model divides a population into susceptible, infected, and recovered individuals, and two parameters characterize the evolution: the transmission rate β and the recovery rate γ. In the simplest version of the model, β and γ are assumed to be constant on the epidemic time scale. The time evolution of the fractions (S, I, R) of susceptible, infected, and recovered agents is then given [5,7] by

$$\begin{aligned} \dot{S} &= -\beta SI, \\ \dot{I} &= \beta SI - \gamma I, \\ \dot{R} &= \gamma I. \end{aligned} \tag{1}$$

This system of differential equations was studied in detail during the past century [5,7,8]; in particular, explicit solutions describing the beginning of epidemics [3], and complete implicit solutions [9–11], have been derived.

Even though the basic SIR model has been successful, it can be considered too simplistic. This is why more accurate variants [12–16] and a number of more complex models [7,17–20] have since been introduced. Among these models, compartment models on networks provide a good balance between simplicity, physical understanding, and improved accuracy [16,21–28]. This approach benefited both from the wealth of activity in network theory in the past two decades and from the increased availability of large amounts of data [29] about contact networks (see [30,31] for a complete review on the subject). This has resulted in a steady increase of papers published on the subject of epidemics on networks since the year 2000 [32].

Despite their success in extending the basic SIR model, these network models so far lack one important feature, which is the existence of analytical solutions for the models' equations. The importance and usefulness of these analytical results should not be underrated, as they provide a much deeper understanding of the mechanisms at work than can be achieved numerically. Moreover, they constitute a benchmark for more complex models where no analytical solution is available. Our goal here is to provide such analytical results in the case of random homogeneous networks, which are characterized by their constant connectivity k. For any given value of k we obtain analytic expressions analogous to (and in some circumstances stronger than) the ones existing for the SIR model (1); when $k = 2$ or 3 we obtain simple explicit expressions, while in the limit $k \to \infty$ we recover the basic SIR, leading to some new physical insights as well as some useful approximations of this well-known model.

The article is organized as follows. In Sec. II, we present the SIR model on a random homogeneous network with k neighbors, called the SIR-k model, and its dynamic equations. In Sec. III, we derive the (implicit) analytical solution of these equations. We then study the impact of our results on the epidemic threshold, and the case of a small number of neighbors, which provides more explicit expressions. In Sec. IV, we focus on the limiting case $k \to \infty$ to derive the exact solution of the SIR model. We then derive some significant approximations with simpler expressions and study the consequences of our results on the epidemic's peak time. Finally, concluding remarks are gathered in Sec. V.

II. SIR MODEL ON A RANDOM HOMOGENEOUS NETWORK WITH k NEIGHBORS

We consider a population of N individuals who can be in one of the three possible states (susceptible, infected, recovered). Each agent is in contact with k fixed neighbors only. These neighbors are chosen randomly among the population. The standard SIR model, where everyone is in contact with everyone, corresponds to the large-k limit of this model. The population can be represented by a random homogeneous network with fixed connectivity k, where each node corresponds to an individual and edges connect neighboring individuals. Associated with each of these edges is a probability λdt that an infected individual will infect a (susceptible) neighbor during the time interval $[t, t+dt[$. As in the basic SIR model, infected individuals may also recover from the disease during that time interval with a probability γdt. The epidemic then spreads through the network following a standard Markovian process (see [33] for a detailed procedure), and dynamic quantities are averaged over realizations of the network and of the Markovian process.

The time evolution of the average fractions $S(t)$, $I(t)$, and $R(t)$ of susceptible, infected, and recovered individuals requires taking into account correlations between the states of two neighbors, which are very strong in a network. For a SIR model on a k-homogeneous network we obtain the system of equations

$$\dot{S} = -\lambda k G^{si} S, \tag{2a}$$

$$\dot{I} = \lambda k G^{si} S - \gamma I, \tag{2b}$$

$$\dot{R} = \gamma I, \tag{2c}$$

with $S(t)+I(t)+R(t)=1$. Here, $G^{si}(t)$ corresponds to the probability that a neighbor of a given susceptible individual is itself infected; thus $kG^{si}(t)$ is the average number of infected individuals in the neighborhood of a susceptible individual. Introducing $G^{ss}(t)$ and $G^{sr}(t)$ in a similar way, with $G^{ss}(t)+G^{si}(t)+G^{sr}(t)=1$, the time dependence of these two-point correlators is given by

$$[S\dot{G}^{ss}] = -2SG^{ss}(k-1)G^{si}\lambda, \tag{3a}$$

$$[S\dot{G}^{si}] = SG^{ss}(k-1)G^{si}\lambda, -SG^{si}[(k-1)G^{si}+1]\lambda - \gamma SG^{si} \tag{3b}$$

$$[S\dot{G}^{sr}] = \gamma SG^{si} - SG^{sr}(k-1)G^{si}\lambda. \tag{3c}$$

To derive (3) we made the degree pairwise approximation [34], that is, we neglected three-point correlations (and beyond) which should appear in the evolution of G^{si}. Within this approximation, the derivation can be sketched as follows. We note first that $XG^{xy}(t)$ corresponds to the probability for a given edge (here, considered oriented, with the starting vertex being in state x and the arrival vertex being in state y) to be in the state x—y at t. Consider first the case $x=y=s$ and a given edge s—s. For an agent located at one end of this edge to be infected, it is necessary that one of its $(k-1)$ other neighbors be infected and transmit the disease. If we neglect the three-point correlations (between the initial node, its neighbor, and the second neighbors), each of the other neighbors has a probability G^{si} to be infected, and in that case, a probability λdt to transmit the disease. Thus, the time evolution of SG^{ss} is given, at order dt, by Eq. (3a) (the factor 2 accounts for the two ends of edge s—s). Equation (3b) can be explained in a similar way; SG^{si} corresponds now to the number of edges, starting from a susceptible node to an infected one. See [35] for a more detailed derivation. This approximation has been for example used in [31] to derive equations for the SI model on a generic network.

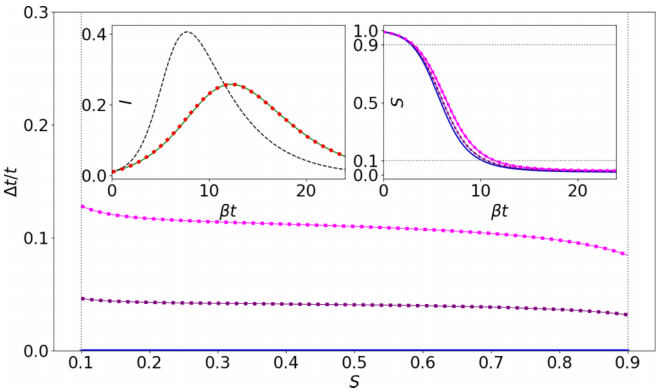

FIG. 1. Main panel: Time delay $\Delta t = t(S) - t_{\mathrm{SIR}}(S)$ with t_{SIR} obtained by numerically solving (1). Solid thick dark blue: analytical expression (26), corresponding to the limit case SIR-∞, yielding 0 as expected. Purple ($k=50$) and magenta ($k=20$) plots: numerical resolution of the SIR-k model (2) (solid lines) and corresponding analytical solution (11) (dots). Right inset: proportion of susceptible $S(t)$ for the same configurations. The gray horizontal dotted lines indicate the range of S values taken for the main panel. Left inset: proportion of infected $I(t)$ for $k=5$. Red dotted line: numerical resolution of the SIR-5 model Eqs. (2) and (3); green solid line: average over 100 realizations of the Markovian process of an epidemic on a large homogeneous network of degree $k=5$, with $N=3000$ nodes (with random initial infected nodes); black dashed line: basic SIR model with $\beta=\lambda k$. Parameters are $\mu=0.25$, $S_0=0.99$.

Our approximation by comparing a numerical solution of Eqs. (2) and (3) with a Markovian evolution of a population according to the same dynamics. The parameters of our problem are S_0 the initial proportion of susceptible agents, k the number of neighbors, $\beta=\lambda k$ the contagiousness and γ the recovery rate, which leads to a dimensionless quantity $\mu=\gamma/\beta$ driving the epidemic, while β only changes the time scale (see for example [10]).

In the case of homogeneous networks with a large number of nodes $N\to\infty$, as we consider here, the fraction of loops with arbitrary finite size vanishes [36–38]. Therefore, the correlations beyond two-point ones can be neglected and the degree pairwise approximation becomes exact in this limit [39]. Equations (2) and (3) form what we will call the "SIR-k model" in the following. In Fig. 1 (left inset), we demonstrate the accuracy of

III. ANALYTICAL SOLUTION OF THE SIR-k EQUATIONS

A. General expression

From Eqs. (2) and (3), we can obtain an ordinary differential equation involving only $S(t)$. Inserting $G^{si} = -\dot{S}/(\beta S)$, which we get from Eq. (2a), into Eq. (3a), we have

$$\frac{[S\dot{G}^{ss}]}{SG^{ss}} = 2\frac{k-1}{k}\frac{\dot{S}}{S}. \tag{4}$$

At $t = 0$, $S(0) = S_0 = G^{ss}(0)$ if we assume that there are no correlations at time 0 (i.e., the neighborhood of infected and susceptible individuals is the same), then Eq. (4) can be integrated as $G^{ss} = S_0^{\frac{2}{k}} S^{1-\frac{2}{k}}$. Using Eq. (2a) and this expression for G^{ss}, Eq. (3b) yields

$$\ddot{S} = \lambda S_0^{\frac{2}{k}} S^{1-\frac{2}{k}}(k-1)\dot{S} + \frac{k-1}{k}\frac{\dot{S}}{S} - (\gamma+\lambda)\dot{S}. \tag{5}$$

This is a second-order differential equation in S that we need to integrate twice. A first integration is obtained by dividing (5) by $\dot{S}$ and introducing $\varphi(S) = \dot{S}$, which verifies

$$\frac{d\varphi(S)}{dS} = \lambda S_0^{\frac{2}{k}} S^{1-\frac{2}{k}}(k-1) + \frac{k-1}{k}\frac{\varphi(S)}{S} - (\gamma+\lambda). \tag{6}$$

Equation (6) can be integrated as an equation in the variable S to give

$$\varphi(S) = kS_0^{2/k}\lambda S^{2(1-\frac{1}{k})} - k(\lambda+\gamma)S + C_1 S^{1-\frac{1}{k}}, \tag{7}$$

where C_1 is given by the initial conditions: $C_1 = \dot{S}(0)S_0^{-1+1/k} - \lambda k S_0^{1+1/k} + k(\lambda+\gamma)S_0^{1/k}$. Using $\dot{S}(0) = -\lambda k S_0(1-S_0)$, this constant reduces to $C_1 = k\gamma S_0^{1/k}$. Changing to the variable $z \equiv (S/S_0)^{\frac{1}{k}}$, and using $\mu = \gamma/\beta$, we obtain

$$\dot{z} = \lambda P(z), \quad P(z) = S_0 z^{k-1} - (k\mu+1)z + k\mu. \tag{8}$$

Separating the variables z and t and using the partial fraction decomposition of $1/P(z)$ in terms of the roots z_j ($j = 0, \ldots, k-2$) of $P(z)$, the integral of Eq. (8) becomes

$$\int_1^z \frac{dz'}{P(z')} = \sum_{j=0}^{k-2} \int_1^z \frac{A_j}{z'-z_j} dz' = \lambda t, \tag{9}$$

with

$$A_j = \frac{1}{P'(z_j)} = \frac{1}{\prod_{l\neq j}(z_j - z_l)}. \tag{10}$$

Equation (9) readily gives an explicit expression for t as a function of S as

$$t(S) = \frac{1}{\lambda}\sum_{j=0}^{k-2} A_j \ln\left(\frac{(S/S_0)^{1/k} - z_j}{1-z_j}\right). \tag{11}$$

Note that the complex roots z_j are pairwise complex conjugate so that the whole sum is real, as it should be. One then gets a parametric solution for the number of infected individuals under the form $(t(S), I(S))$ by integrating Eq. (2b). Indeed, since $S(t)$ is monotonous, Eq. (2b) can be rewritten as

$$\frac{dI}{dS} = -1 - \gamma I \frac{dt}{dS}, \tag{12}$$

which upon integration yields

$$I(S) = \left(1 - S_0 - \int_{S_0}^{S} e^{\gamma t(s')} ds'\right) e^{-\gamma t(S)}. \tag{13}$$

The maximum of I corresponds to the value of S where $dI/dS = 0$, that is,

$$I(S)\frac{dt}{dS} = -\frac{1}{\gamma}, \tag{14}$$

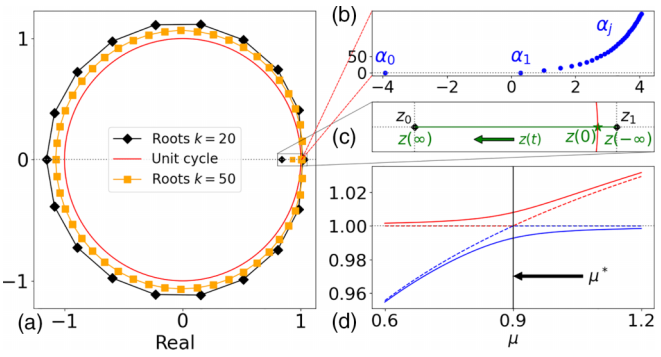

FIG. 2. (a) Orange squares (resp. black diamonds): location, in the complex plane, of the roots of the polynomial $P(z)$ Eq. (8) for $k = 50$ (resp. $k = 20$) with $S_0 = 0.8$ and $\mu = 0.25$. (b) Blow-up showing, in the complex plane, the limit as $k \to \infty$ of the α_j defined by $z_j = 1 + \alpha_j/k$. The complex z_j (and thus the complex α_j) come in conjugate pairs. (c) Zoom on the complex plane close to 1 with $z(t) = (S(t)/S_0)^{1/k}$ traveling the green line from $z_1 = z(-\infty)$ to $z_0 = z(\infty)$ and passing through $z(0) = 1$. (d) Blue line (resp. red line): illustration, for $k = 20$, of the variation with μ of the roots $z_0(\mu)$ (resp. $z_1(\mu)$) for $S_0 = 0.99$ (solid line) and $S_0 = 1$ (dashed line). The value μ_k^* such that $z_0(\mu_k^*) = z_1(\mu_k^*) = 1$ is the epidemic threshold.

with $t(S)$ explicitly given by (11), while the calculation of $I(S)$ involves a single numerical integral over S.

We checked for many different values of the parameters (S_0, μ, k) that the analytical solution (11) perfectly reproduces the numerical resolution of (2) and (3), and we illustrate it for one example in Fig. 1. Note that a similar approach allows us to address the SI model, which corresponds to the limit $\mu \to 0$; in that case we get

$$S(t) = S_0^{-\frac{2}{k-2}}\left(\frac{1-S_0}{S_0}e^{\lambda(k-2)t} + 1\right)^{-\frac{k}{k-2}}, \tag{15}$$

which in the limit $k \to \infty$ coincides with the known solution of the SI model [7].

B. Epidemic threshold

We now comment on the consequences of Eq. (11). Polynomials such as $P(z)$ in Eq. (8) have a long history, dating back to Lambert [40,41] and Euler [42]. In particular, one can explicitly express all the roots z_j as an infinite series (see [43,44]). As illustrated in Fig. 2(a), for $k > 2$ there are two real positive roots, $z_0 \in [0, 1]$ and $z_1 \in [1, \infty[$. Since $S/S_0 \in [0, 1]$, the only possible divergence of t in (11) corresponds to the root z_0, and we thus get that $S_\infty \equiv \lim_{t\to\infty} S(t) = S_0 z_0^k$. A useful quantity for public agencies in charge of controlling the epidemic (see [8] for the basic SIR model) is the fraction of the population that will be infected during the course of the epidemic; it can be expressed as $\mathcal{I}_{\text{tot}}^{(k)} = S_0 - S_\infty = S_0(1 - z_0^k)$. The second positive real root z_1 can then be interpreted as the nonphysical limit to which S would tend if one follows the SIR-k equations for negative times, $S_{-\infty} \equiv \lim_{t\to-\infty} S(t) = S_0 z_1^k > 1$. As illustrated in Fig. 2(c), the associated quantity $z(t) = (S(t)/S_0)^{1/k}$ decreases from 1 to z_0 for $t \in [0, +\infty[$, and from z_1 to 1 for the non-physical part $t \in]-\infty, 0]$.

Whatever the value of μ and k, $P(1) = S_0 - 1$. Thus, as illustrated in Fig. 2(d), $z = 1$ cannot be a root of $P(z)$ for $S_0 < 1$, but always is for $S_0 = 1$. In the latter case, two situations can occur. The first one would be that $z_1 = 1$ and $z_0 < 1$, in which case an epidemic starting with $S_0 = 1$ (i.e., with an infinitesimal fraction of infected individuals) would eventually propagate into the network and infect a finite fraction of the population. Introducing the time t_0 corresponding to the constant term in Eq. (11), namely

$$t_0 = -\frac{1}{\lambda}\sum_{j=0}^{k-2} A_j \ln|z_j - 1| \underset{S_0\to 1}{\sim} \frac{\ln(1-S_0)}{\lambda(2+k(\mu-1))}, \tag{16}$$

we see that $\lim_{S_0\to 1} t_0 = \infty$. This expresses the fact that the beginning of the epidemic takes an infinite amount of time as the initial proportion of infected individuals goes to zero. The other possibility, $z_0 = 1$ and $z_1 \geqslant 1$, corresponds to $S_\infty = 1$: an epidemic starting with $S_0 = 1$ does not propagate. The value μ_k^* of the parameter μ corresponding to the transition between these two regimes is the threshold beyond which, for $S_0 = 1$, the epidemic does not spread. At the threshold, $z = 1$ is a double root of $P(z)$ and thus $\mu_k^* = (k-2)/k$.[1] As $k \to \infty$ we get $\mu_k^* \to 1$, which coincides with the result of Kermack and McKendrick [3] for the original SIR model.

C. Small number of neighbors

It is possible to invert the expression (11) for $k = 2$ and 3. First, consider the case $k = 2$. A random network of size N then corresponds to a set of disconnected loops of different sizes. In the $N \to \infty$ limit, however, all but a negligible proportion of agents would belong to a large loop, and the average quantities we consider here, for example in Eqs. (2) and (3), behave in the same way within a random network or within a single connected loop. Furthermore, there is only one root $z_0 = 2\mu/(I_0 + 2\mu)$, with $I_0 = 1 - S_0$ the initial fraction of infected individuals. We can therefore write (11) as

$$t(S) = \frac{1}{\lambda} A_0 \ln\left(\frac{(S/S_0)^{1/2} - z_0}{1 - z_0}\right), \tag{17}$$

with $A_0 = -1/(I_0 + 2\mu) < 0$. Inverting Eq. (17) we get

$$S(t) = S_0\left[1 + \frac{I_0(e^{-t/\tau} - 1)}{I_0 + 2\mu}\right]^2, \quad \tau = \frac{1}{\lambda(2\mu + I_0)}. \tag{18}$$

$S(t)$ thus follows an exponential decay with rate τ and converges to $S_\infty = S_0 z_0^2$, as expected. We get $\mathcal{I}_{\text{tot}}^{(2)} = S_0(1 - (1 - I_0/(2\mu))^{-2})$, which varies from S_0 for strong epidemic $I_0/\mu \gg 1$ to 0 with $I_0/\mu \ll 1$. In particular, $\lim_{S_0\to 1} \mathcal{I}_{\text{tot}}^{(2)} = 0$ for any positive value of μ, which can also be seen from the fact that $\mu_2^* = (k-2)/k = 0$. This is unique to the $k = 2$ case because of its essentially 1d geometry, which implies that the number of infected agents caused by a single patient zero is necessarily finite.

[1]This expression for the threshold can be derived also from the results in Sec. III C of [28]

For the case $k = 3$, we get $P(z) = S_0 z^2 - (3\mu + 1)z + 3\mu$, which has two (real positive) roots,

$$z_{0,1} = \frac{1}{2S_0}[(3\mu + 1) \pm \sqrt{(3\mu + 1)^2 - 12\mu S_0}], \tag{19}$$

yielding

$$t(S) = \frac{A_0}{\lambda} \ln\left[\frac{((S/S_0)^{1/3} - z_0)(1 - z_1)}{((S/S_0)^{1/3} - z_1)(1 - z_0)}\right], \tag{20}$$

where we have used that $A_1 = -A_0 = 1/(z_1 - z_0)$. We can invert Eq. (20) to get

$$S(t) = S_0\left(\frac{z_0 - z_1 B e^{\lambda(z_0 - z_1)t}}{1 - B e^{\lambda(z_0 - z_1)t}}\right)^3, \quad B = \frac{1 - z_0}{1 - z_1}. \tag{21}$$

As expected, this expression verifies that $S(0) = S_0$ and $S_\infty = S_0 z_0^3$. The explicit expression for $\mathcal{I}_{\text{tot}}^{(3)}$ is $S_0 - \frac{1}{8S_0^2}[(3\mu + 1) + \sqrt{(3\mu + 1)^2 - 12\mu S_0}]^3$. For $S_0 = 1$, the roots simplify to $z_0 = \min(1, 3\mu)$, $z_1 = \max(1, 3\mu)$, and we recover $\mu_3^* = \frac{1}{3}$; for $\mu < \mu_3^*$, $\mathcal{I}_{\text{tot}}^{(3)} = 1 - (3\mu)^3$, while for $\mu \geqslant \mu_3^*$ the epidemic does not propagate as $S_\infty = 1$.

Finally, we consider the case $k = 4$, but limiting ourselves for simplicity to the limit $S_0 \to 1$ and the regime $\mu < \mu_4^* = 1/2$. In that case, $P(z)$ has three roots, which, introducing $\kappa = \sqrt{1/4 + 4\mu}$, can be written as $z_0 = \kappa - \frac{1}{2}$, $z_1 = 1$, $z_2 = -\kappa - \frac{1}{2}$ with furthermore $A_0 = [\kappa(2\kappa + 3)]^{-1}$, $A_1 = [2 - 4\mu]^{-1}$, $A_2 = [\kappa(2\kappa - 3)]^{-1}$. The epidemics propagate only if $z_0 < 1$, that is if $\mu < \mu_4^* = 1/2$, in which case, scaling out the time t_0 introduced in Eq. (16), the dynamics is described by

$$t - t_0 = \frac{1}{\kappa\lambda}\sum_{\epsilon=\pm 1}\left(\frac{1}{2\kappa + 3\epsilon} \ln\left|\frac{S^{1/k} + \epsilon\kappa + \frac{1}{2}}{S^{1/k} - 1}\right|\right), \tag{22}$$

and $\mathcal{I}_{\text{tot}}^{(4)} = (-16\mu^2 - 8\mu + 1/2) + (1 + 8\mu)\sqrt{4\mu + 1/4}$ (which is indeed such that $\mathcal{I}_{\text{tot}}^{(4)}(\mu_4^*) = 0$).

IV. LARGE $-k$ LIMIT OF THE SIR $-k$ MODEL

A. Exact expression

Another interesting limit of the SIR-k model is $k \to \infty$, through which we recover the original SIR model, but with a new point of view. As illustrated in Fig. 2, z_0 and z_1 converge to 1 (from below and from above, respectively) and all the other roots converge to the unit circle in the complex plane. This can be understood from their series expansion in [43,44]. Using that z_j is a root of $P(z)$, we can write the factor A_j defined in Eq. (10) as

$$A_j = \left[(k-1)k\mu\frac{z_j - 1}{z_j} - k(\mu - 1) - 2\right]^{-1}. \tag{23}$$

For most roots of $P(z)$, $z_j - 1 = O(k^0)$ (we refer to them as "far from one") and thus $A_j = O(k^{-2})$. It is only for the roots close to one, and more precisely such that $z_j - 1 = O(k^{-1})$, that $A_j = O(k^{-1})$. In the same way, the logarithm factors are $O(k^{-1})$ for the roots far from one and $O(k^0)$ for the roots close to one. In Eq. (11), noting that $\lambda^{-1} = k\beta^{-1}$, we see that the sum over roots far from one involves $O(k)$ terms of order $O(k^{-2})$ and has therefore a negligible $O(k^{-1})$ contribution,

whereas each root close to one has an $O(k^0)$ contribution. We can thus write all relevant roots as $z_j = 1 + \alpha_j/k$ where α_j reaches a constant value as $k \to \infty$. Writing that z_j is a root of $P(z)$ thus reads

$$S_0\Big(1+\frac{\alpha_j}{k}\Big)^{k-1} = k\mu\left[\left(1+\frac{1}{k\mu}\right)\left(1+\frac{\alpha_j}{k}\right)-1\right], \quad (24)$$

which, taking the limit $k \to \infty$ on both sides (with α_j now corresponding to that limit), gives $\exp(\alpha_j) = (\mu/S_0)(1/\mu + \alpha_j)$. Defining now $\gamma_j = \alpha_j + 1/\mu$ and $\chi = (S_0/\mu)e^{-1/\mu}$, we get

$$\chi = \gamma_j \exp(-\gamma_j). \quad (25)$$

Equation (25) can be rewritten in terms of the Euler T function (see [41] for mathematical details) as $\gamma_j = T(\chi)$. The T function has two real branches T_0 and T_{-1} which correspond to the two positive real roots of $P(z)$, and an infinite number of complex branches corresponding to the complex numbers γ_j. In particular, we get for the first root $\lim_{k\to\infty} S_\infty = \mu T_0(\chi)$, which is equivalent to the well-known self-consistent equation $S_\infty = 1 + \mu \ln(S_\infty/S_0)$ given, for instance, in [4]. Taking the large-k limit in Eqs. (23) and (11), together with $\beta = \lambda k$ and the expression of the relevant $z_j = 1 + \frac{\alpha_j}{k}$, leads to

$$\beta\, t(S) = \frac{1}{\mu}\sum_{j=-\infty}^{\infty} \frac{1}{\alpha_j + 1/\mu - 1} \ln\left(1 + \frac{\ln(S_0/S)}{\alpha_j}\right),$$
$$\alpha_j = T_{-j}(\chi) - 1/\mu, \quad (26)$$

where the complex quantities α_j are pairwise complex conjugate (T_{-2} is conjugate with T_1, T_{-3} with T_2, etc.) so that the whole sum is real. In Fig. 1, we check the accuracy of this expression.

B. Approximate expression for $t(S)$

An implicit analytical solution $t(S)$ for the SIR model (1) is known in the literature and takes the form of an integral (see, for instance, [9]). Our formula (26) is an alternative expression for $t(S)$ and comes with interesting new insights, as it depends on quantities α_j, which have an explicit expression. In Fig. 2, we show the first terms of the sequence. We see that $\alpha_0 < 0$ and $\alpha_1 > 0$ are indeed the two unique real values, while the subsequent α_j are purely complex; the latter are well approximated by $\alpha_j \simeq 2\pi i j$ for large (possibly negative) j as the roots z_j converge to the unit circle $\exp(\frac{2\pi i j}{k-2})$. Therefore, for m sufficiently large, the contributions of the terms $j \geqslant m$ of Eq. (26) can be approximated by

$$\frac{2}{\mu}\Re\left[\sum_{j=m}^{\infty}\frac{\ln\left(1-\frac{1}{\alpha_j}\ln(S/S_0)\right)}{\alpha_j+1/\mu-1}\right]$$
$$\simeq -\frac{2\ln(S/S_0)}{(2\pi)^2\mu}\int_m^\infty \frac{1}{\alpha_j^2}dj \simeq \frac{2\ln(S/S_0)}{(2\pi)^2\mu}\frac{1}{m}, \quad (27)$$

in which we use that $\alpha_j + 1/\mu - 1 \simeq \alpha_j$ which is valid as long as $2\pi j \gg 1/\mu$, and which becomes quickly negligible as m increases if μ is not too small.

Further understanding of the qualitative behavior of the sum Eq. (26) can be obtained, noting that the effective reproduction number $R_{\text{eff}} = S/\mu$ has to be larger than 1 for the epidemic to propagate. One can therefore assume $\mu \in [0, 1]$ and S_0 in the interval $[\mu, 1]$. Thus, for μ not too far from 1 and using $\delta\mu = (1-\mu)$ as a small parameter, we can in any case assume $\delta S_0 = (1 - S_0) < \delta\mu$. In practice, however, we think of the initial time $t = 0$ as a situation where most agents are susceptible, only a very small fraction is infected, and nobody has recovered yet. In most of the concrete cases, and for essentially all the illustrations, we shall consider below $\delta S_0 \ll \delta\mu$, and we shall assume that at worse $\delta S_0 = O(\delta\mu^2)$. In that case, one can show (see Appendix A 3) that at all times $\delta S = (1 - S) = O(\delta\mu)$, implying also that $\ln(S_0/S) = O(\delta\mu)$.

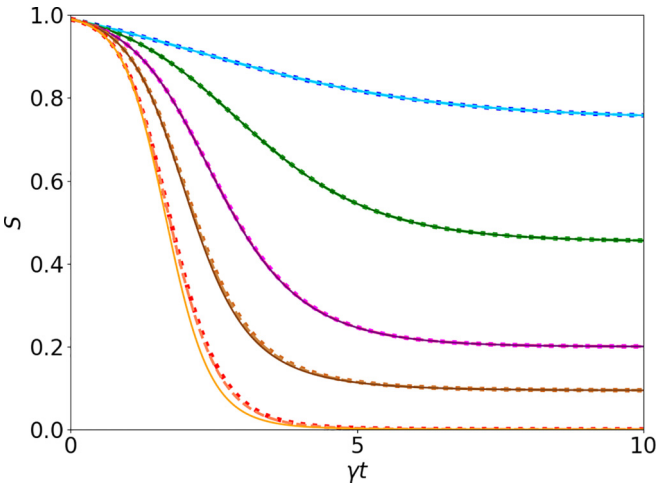

FIG. 3. Comparison of exact S (solid lines) with approximation Eq. (28) at first and second order in $\delta\mu = (1-\mu)$ (dotted and dashed lines respectively). $S_0 = 0.99$ is fixed and μ evolve from 0.1 to 0.9 : ($\mu = 0.1$, red), ($\mu = 0.3$, brown), ($\mu = 0.5$, magenta), ($\mu = 0.7$, green), ($\mu = 0.9$, blue). Although Eq. (28) is formally an expansion near $\mu = 1$, we see that its validity extends in practice in the whole range of μ, except in the neighborhood of 0.

Noting (cf. Appendix A) that at $\alpha_0(\mu=1) = \alpha_1(\mu=1) = 0$, when for $j \geqslant 2$ $\alpha_j^0 := \alpha_j(\mu=1) \neq 0$, this means that the contribution of the two first terms $j = 0, 1$ are $O(\delta\mu^0)$, when all the higher j contributions are $O(\delta\mu)$. We thus have

$$\beta t(S) = \frac{1}{\mu}\left[\sum_{j=0,1}\frac{\ln\left(1+\frac{1}{\alpha_j}\ln(S_0/S)\right)}{\alpha_j+1/\mu-1} - 2\mathcal{K}^{(0)}\ln(S_0/S) + O(\delta\mu^2)\right], \quad (28)$$

with $\mathcal{K}^{(0)} := \Re(\sum_{j=2}^{\infty}(\alpha_j^0)^{-2}) \simeq -0.028$ a, fairly small, pure number. As illustrated in Fig. 3, the approximation Eq. (28) is actually very accurate on a significant portion of the range [0, 1], and this range can be even further extended by computing the $O(\delta\mu^2)$ correction to Eq. (28) (cf. Appendix A).

C. Epidemic peak time

As mentioned, an important quantity in the context of an epidemic breakout is the epidemic peak time, which, using the fact that, for SIR, the epidemic peak $dI/dt = 0$ implies

$S = \mu$, can be obtained as $t_{\rm peak} = t(S{=}\mu)$, and for which even a leading order approximation is presumably useful.

For μ sufficiently close to 1, this can be obtained starting from Eq. (28), neglecting the $-2\mathcal{K}^{(0)}\ln(S_0/S)$ correction, and evaluating α_0 and α_1 to leading order in $\delta\mu$. This calculation is performed in Appendix B, leading to Eq. (B1). From this we get

$$\beta t_{\rm peak} \simeq \frac{1}{p}\left[\ln\left(1-\frac{\ln(S_0/\mu)}{\delta\mu - p}\right) - \ln\left(1-\frac{\ln(S_0/\mu)}{\delta\mu + p}\right)\right], \tag{29}$$

with $p = \sqrt{2\delta S_0 + \delta\mu^2}$, valid for $\delta\mu = (1-\mu)$ small ($\delta S_0 = (1-S_0) < \delta\mu$, and possibly $\ll \delta\mu$).

For μ a bit further away from 1, where this approximation starts to degrade, it turns out that a better approximation of $t_{\rm peak}$ can be obtained following the same approach but using the $\mu \to 0$ expansion of α_0 and α_1. We get (see Appendix B2)

$$\beta t_{\rm peak} \simeq \frac{1}{\mu}\left[\frac{\ln\left(1-\frac{\ln(\mu/S_0)}{\chi+\chi^2-1/\mu}\right)}{\chi+\chi^2-1} + \frac{\ln\left(1-\frac{\ln(\mu/S_0)}{(1-S_0)/(S_0-\mu)}\right)}{(1-S_0)/(S_0-\mu)+1/\mu-1}\right],$$
$$\chi = (S_0/\mu)e^{-1/\mu}. \tag{30}$$

An expansion for $\mu \ll 1$ can finally be obtained from the integral form of $t(S)$ given in [9], and leads to (cf. Appendix B1)

$$\beta t_{\rm peak} \simeq \ln\left(\frac{S_0}{1-S_0}\right) - \ln\mu - \mu\left(1+\ln(1-S_0) - \frac{1}{2}\ln^2\frac{S_0}{\mu} - {\rm Li}_2(S_0)\right), \tag{31}$$

with Li_n the polylogarithm function.

In Fig. 4, we compare the predictions in Eqs. (29), (30), and (31) with the exact $\beta t_{\rm peak}$, demonstrating that, with $S_0 \geqslant 0.999$, the full range of $\mu \in [0,1]$ is covered with these three regimes.

Equations (29), (30), and (31), corresponding respectively to large, intermediate, and small μ, provide explicit expressions and physical indications of how one can delay the epidemic peak in practice. Let us assume that the parameter γ which characterizes the rate of recovery from the illness is given by biological factors, and thus fixed, but that the transmission rate β can be modified by nonpharmaceutical interventions such as wearing masks or limiting contact between people. We thus assume that μ can be modified, but that this is done with $\beta\mu = \gamma$ constant.

First, we see in Fig. 4 that the curve $\beta t_{\rm peak}(\mu)$ is rather flat in the range $\mu \in [0.05, 0.5]$, implying that $t_{\rm peak}$ is essentially proportional to $1/\beta$ for $\mu < 0.5$. Then, different kinds of corrections appear in the different regimes. The most useful formula is presumably Eq. (30), which provides a compact and explicit analytical result (with only two terms), in a regime that corresponds to most of the practical use ($2 \leqslant R_0 \leqslant 5$).

As a practical example, starting with $S_0 = 0.99$ and applying restrictive measures to change $\mu = 0.25$ to $\mu = 0.5$ (which means changing R_0 from 4 to 2) would allow reducing $t_{\rm peak}$ by a factor of 2.25 according to Eq. (30), while the exact reduction factor is 2.18, with very similar absolute values. For $S_0 = 0.9$, this factor is only 1.61, according to Eq. (30), while the exact value is 1.57. We therefore have a precise indication about $t_{\rm peak}$ from a very simple expression, which does not require any knowledge of the Lambert function and does not involve the computation of an integral. This makes it possible to analyze qualitatively why early detection of the epidemic is important, as restrictive measures to delay the peak will be significantly less efficient for an epidemic that has already spread significantly in the population.

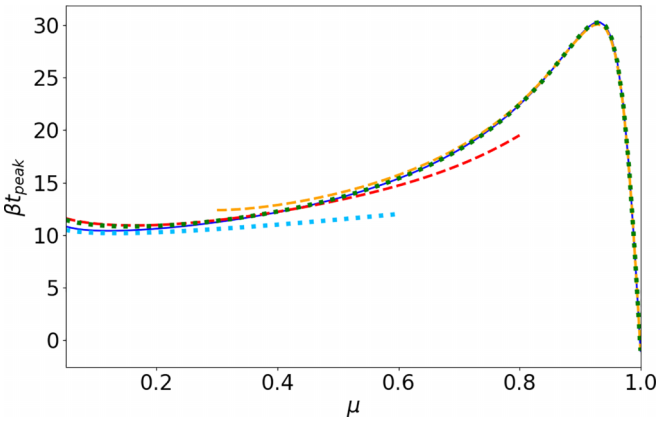

FIG. 4. Comparison of the exact $\beta t_{\rm peak}(\mu)$ (blue solid line) with different approximations, for a fixed $S_0 = 0.999$ and $\mu \in [0.05, 1]$. Cyan dotted line: approx. (31) which works at small μ. Red dashed line: approx. (30) which is rather valid for small and intermediate μ. Orange dashed line: approx. (29) for μ close to 1 and also for intermediate μ. Dotted green line: approximation obtained from Eq. (28) with $S = \mu$, which match the exact $t_{\rm peak}(\mu)$ extremely well except for very small μ's. The regimes of validity of the different approximations improve as $S_0 \to 1$, and would somewhat degrade as δS_0 increases.

V. CONCLUSION

In this work, we have derived Eqs. (2) and (3) for the SIR-k model, and obtained an exact implicit expression of $t(S)$ (11), valid for arbitrary k, as a finite sum over the roots z_j of the polynomial $P(z)$ (8).

It turns out that the main qualitative properties of the epidemic dynamics are governed by its two positive real roots (z_0, z_1). In particular, the proportion of agents infected during the total duration of the epidemic is given by $\mathcal{I}_{\rm tot}^{(k)} = S_0(1 - z_0^k)$, for which we have an explicit formula both for small and very large k. Taking $S_0 = 1$, i.e., assuming a negligibly small initial proportion of infected agents (for easier reading), we got $\mathcal{I}_{\rm tot}^{(3)} = 1 - (3\mu)^3$ for $k = 3$, while for the SIR model limit, we obtained $\mathcal{I}_{\rm tot}^{(\infty)} = 1 - \mu T_0(\chi) \simeq 1 - \mu\chi = 1 - e^{-1/\mu}$. Thus, for small μ (contagious diseases), the larger k, the more virulent the epidemic, as $\mathcal{I}_{\rm tot}^{(\infty)}$ will converge faster to 0 with $\mu \to 0$ than $\mathcal{I}_{\rm tot}^{(k)}$.

The values of the real roots (z_0, z_1) also affect the threshold value of μ for which, even for an infinitely small initial proportion of infected individuals, an epidemic starts to propagate

and affect a finite proportion of the agents. This threshold is given by the condition $z_0(\mu_k^*) = z_1(\mu_k^*) = 1$, leading to $\mu_k^* = (k-2)/k$. This value is lower than its counterpart for the basic SIR model $\mu_{\rm SIR}^* = \mu_\infty^* = 1$, which indicates that the propagation of epidemics is more difficult in the SIR-k model than in the basic SIR one, in agreement with the final epidemic size, which is also lower for the SIR-k model. This is in contrast with heterogeneous networks, for which an epidemic spreads more easily than in the SIR model.

In the cases $k = 2$ and $k = 3$ we got exact explicit expressions for $S(t)$. In the limit $k \to \infty$, we obtained new exact expressions for the original SIR model, which provides a new point a view, together with useful approximate results for this well-known problem. In particular, Eq. (28) and Fig. 3 demonstrate that for all values of μ except near 0, keeping only the contributions of the real α_j's, i.e., $j = 0, 1$, provide an excellent approximation of $t(S)$. Further approximation for the epidemic peak time Eqs. (29), (30), and (31) are shown in Fig. 4 to work extremely well numerically.

The SIR-k model on homogeneous networks presumably provides a good balance between an increase in complexity and an increase in effectiveness. It is characterized by only three parameters (S_0, μ, k) which, compared with the basic SIR, only adds the parameter k corresponding to the average number of possible contacts of individuals, a relatively accessible quantity in practice. Our SIR-k model is almost as simple as the basic SIR model. Indeed, it benefits from a simpler exact solution than the SIR, while numerical resolution remains fast and tractable (six equations instead of three). We therefore hope that our work will encourage institutions to consider using the SIR-k model in practice, instead of the basic SIR, especially as the two produce significantly different results when the number of neighbors is low, as shown in Fig. 1. Our results pave the way for the analytical study of more realistic social networks, such as heterogeneous networks with the small-world property [21,45].

APPENDIX A: THE $\mu \to 1$ REGIME FOR $t(S)$

We start by rewriting Eq. (26) as

$$\beta\, t(S) = \frac{1}{\mu}\sum_{j=0,1}\frac{1}{\alpha_j + 1/\mu - 1}\ln\left(1+\frac{\ln(S_0/S)}{\alpha_j}\right) + 2\Re\left[\frac{1}{\mu}\sum_{j=2}^{\infty}\frac{1}{\alpha_j + 1/\mu - 1}\ln\left(1+\frac{\ln(S_0/S)}{\alpha_j}\right)\right]. \tag{A1}$$

1. Contribution of the $j \geqslant 2$ to Eq. (A1)

Noting $\delta\mu = (1-\mu) \ll 1$ and $\delta S_0 = (1-S_0) < \delta\mu$, one can show that for $j \geqslant 2$,

$$\alpha_j = -1 + \tau_j + \frac{\tau_j}{\tau_j - 1}\delta S_0 - \delta\mu + O(\delta\mu^2), \tag{A2}$$

with $\tau_j := T_{-j}(1/e) \neq 1, \forall j \geqslant 2$.

Therefore, for $j \geqslant 2$, $\ln(S_0/S)/\alpha_j = O(\delta\mu)$, and in Eq. (A1), we can expand the log as

$$\ln\left[1+\frac{\ln(S_0/S)}{\alpha_j}\right] = \frac{\ln(S_0/S)}{\alpha_j} - \frac{1}{2}\frac{\ln(S_0/S)^2}{\alpha_j^2}.$$

Together with Eq. (A2), this leads, for the contribution of the $j \geqslant 2$ to Eq. (A1), to

$$\frac{2}{\mu}\Re\sum_{j=2}^{\infty}\frac{1}{\alpha_j + 1/\mu - 1}\ln\left(1+\frac{\ln(S_0/S)}{\alpha_j}\right) = \frac{2\ln(S_0/S)}{\mu}[\mathcal{K}^0 + \delta\mu\mathcal{K}^\mu - \delta S_0\mathcal{K}^{S_0} - \ln(S_0/S)\mathcal{K}^{\ln} + O(\delta\mu^3)], \tag{A3}$$

with

$$\mathcal{K}^0 = \Re\sum_{j\geqslant 2}\frac{1}{(\tau_j-1)^2} \simeq -2.8\times 10^{-3}, \tag{A4}$$

$$\mathcal{K}^\mu = \Re\sum_{j\geqslant 2}\left[\frac{1}{(\tau_j-1)^2} + \frac{1}{(\tau_j-1)^3}\right] \simeq -3.0\times 10^{-3}, \tag{A5}$$

$$\mathcal{K}^{S_0} = \Re\sum_{j\geqslant 2}\frac{2\tau_j}{(\tau_j-1)^4} \simeq -3.8\times 10^{-3}, \tag{A6}$$

$$\mathcal{K}^{\ln} = \Re\sum_{j\geqslant 2}\frac{1}{2(\tau_j-1)^4} \simeq 7.7\times 10^{-5}. \tag{A7}$$

These dimensionless numbers are actually rather small, which explains the quality of the approximation (28) in a large range of $\delta\mu$. This is illustrated in Fig. 5.

2. Expansion for α_0 and α_1

For $z \to 1$, we have [41]

$$T_0(z) = 1 - p + O(p^2), \tag{A8}$$

$$T_{-1}(z) = 1 + p + O(p^2), \tag{A9}$$

with $p := \sqrt{2(1-ez)}$ and $z < 1/e$. With $z = \chi = (S_0/\mu)\exp(-1/\mu)$ (implying $z < 1/e$ since $S_0 < 1$ and the function $\frac{1}{\mu}e^{-1/\mu}$ increases over $[0, 1]$ from 0 to $1/e$), we have $ez \simeq 1 - \delta S_0 - \delta\mu^2/2$, and thus

$$p \simeq \sqrt{2\delta S_0 + \delta\mu^2}. \tag{A10}$$

With $\alpha_{0,1} = T_{0,-1}(\chi) - 1/\mu$, we eventually obtain

$$\alpha_0 = -p - \delta\mu, \quad \alpha_1 = +p - \delta\mu. \tag{A11}$$

3. Range of variation of $S(t)$

As t goes from O to ∞, S decreases monotonously from S_0 to $S_\infty = \mu T_0(\chi)$, which following the same reasoning as above, behaves for μ close to one as

$$S_\infty \simeq 1 - p - \delta\mu. \tag{A12}$$

If δS_0 and $\delta\mu$ are of similar magnitude, i.e., if $\delta S_0 = O(\delta\mu)$, this implies $\delta S_\infty = O(\sqrt{\delta\mu})$, which makes the discussion of the size of the neglected terms in Eqs. (28) and (29) somewhat more involved, without changing the main qualitative content

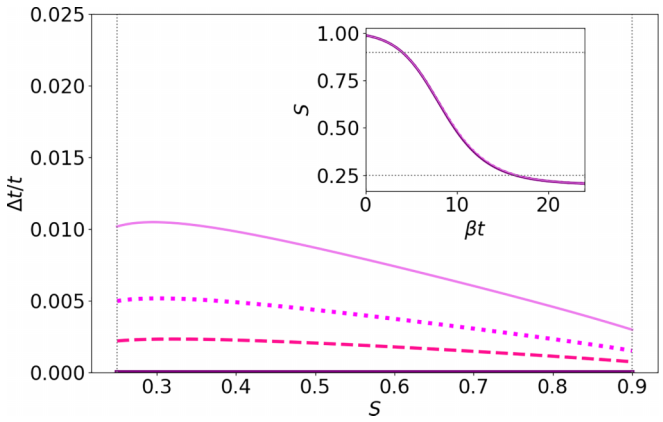

FIG. 5. Main panel: Time delay $\Delta t = t(S) - t_{\mathrm{SIR}}(S)$ with t_{SIR} obtained through analytical expression (26) which has been shown to be exact. Purple solid line: exact expression (26) as a reference. Magenta (Resp. pink) dotted (Resp. dashed) lines: first (Resp. second) order of Eq. (28). Violet solid line: expression (26) with the exact expression of the two real roots only. The gap between this last curve to the first (Resp. second) order curve shows the corresponding correction of these orders. Inset: proportion of susceptible S for the same configurations. The gray horizontal dotted lines indicate the range of S values taken for the main panel comparison (with corresponding vertical lines). Parameters are $\mu = 0.5$, $S_0 = 0.99$, corresponding to the third value of Fig. 3 which is near the standard values ($R_0 \simeq 2$). The discrepancy between the exact curve and the approximation (28) is at most of 0.5%, much lower than the uncertainty that one can expect from μ in practice.

of these equations. On the other hand, if one assumes, as is most of the time the case in practice, δS_0 significantly smaller than $\delta\mu$, and more specifically $\delta S_0 \leqslant O(\delta\mu^2)$, Eq. (A12) implies that $\delta S_\infty = O(\delta\mu)$, and thus $\ln(S_0/S) = O(\delta\mu)$ for all times. We have worked under this assumption in Secs. IV B and IV C and in the Appendixes A1 and B1.

APPENDIX B: EXPLICIT EXPRESSIONS FOR $t(S)$

1. Expansion near $\mu = 1$

With Eq. (A11), the leading order contribution to $t(S)$ as $\mu \to 1$ reads

$$\beta t(S) = \frac{1}{p}\left[\ln\left(1 - \frac{\ln(S_0/S)}{\delta\mu - p}\right) - \ln\left(1 - \frac{\ln(S_0/S)}{\delta\mu + p}\right)\right]. \tag{B1}$$

2. Expansion for intermediate μ

From Fig. 3, and from the discussion in Appendix A1, we see that even if this is formally justified from an expansion near $\mu = 1$, neglecting the contributions of the complex α_js ($j \geqslant 2$) is actually a rather accurate approximation in the whole range of μ except in a small neighborhood of 0. For reasonably small μ, the contribution of the two (remaining) real roots is then rather well described using the Taylor expansion of $T_0(\chi)$ (valid for $\chi \to 0$, thus $\mu \to 0$) given in [41]. We obtain $\alpha_0 \simeq \chi + \chi^2 - 1/\mu$ and $\alpha_1 \simeq (1 - S_0)/(S_0 - \mu)$, from which we get an explicit approximation of $t(S)$

$$\beta t(S) \simeq \frac{1}{\mu}\left[\frac{\ln\left(1 - \frac{\ln(S/S_0)}{\chi + \chi^2 - 1/\mu}\right)}{\chi + \chi^2 - 1} + \frac{\ln\left(1 - \frac{\ln(S/S_0)}{(1-S_0)/(S_0-\mu)}\right)}{(1 - S_0)/(S_0 - \mu) + 1/\mu - 1}\right],$$
$$\chi = (S_0/\mu)e^{-1/\mu}. \tag{B2}$$

Equation (B2), which has been derived assuming μ small (once the contribution of the α_j, $j \geqslant 2$ are neglected), is numerically accurate even for larger values of μ, as illustrated in Fig. 4 for $S_0 = 0.999$ and $\mu \in [0.2, 0.55]$.

3. Small μ expansion

For completeness, we provide here also the small μ expansion of t_{peak}. Starting from the expression in [10], Eq. (10.22), the time t_{peak} for SIR is given (see the discussion below Eq. (10.37) and the one about time rescaling below Eq. (10.6)) by

$$t_{\mathrm{peak}} = \frac{\mu}{\gamma}\int_0^{\ln \mu/S_0} \frac{du}{S_0 e^u - \mu u - 1}. \tag{B3}$$

Changing variables to $v = e^u/\mu$ and expanding the integral gives

$$t_{\mathrm{peak}} = \frac{\mu}{\gamma}\int_1^{\mu/S_0} \frac{dv}{v}\frac{1}{S_0 v - 1 - \mu \ln v} = \frac{\mu}{\gamma}\int_1^{\mu/S_0} \frac{dv}{v}\left(\frac{1}{S_0 v - 1} + \frac{\mu \ln v}{(S_0 v - 1)^2} + O(\mu^2)\right), \tag{B4}$$

which upon integration gives at lowest order

$$\beta t_{\mathrm{peak}} = \left[\ln\left(\frac{S_0}{1 - S_0}\right) - \ln \mu - \mu\left(1 + \ln(1 - S_0) - \frac{1}{2}\ln^2\frac{S_0}{\mu} - \mathrm{Li}_2(S_0)\right)\right], \tag{B5}$$

with Li_n the polylogarithm function.

[1] A. A. Toda, Susceptible-infected-recovered (SIR) dynamics of Covid-19 and economic impact, Covid Economics(1), 43 (2020).

[2] J. D. Osofsky, H. J. Osofsky, and L. Y. Mamon, Psychological and social impact of Covid-19, Psychol. Trauma: Theory Res. Pract. Policy **12**, 468 (2020).

[3] W. O. Kermack and A. G. McKendrick, A contribution to the mathematical theory of epidemics, Proc. R. Soc. Lond. A **115**, 700 (1927).

[4] H. W. Hethcote, The mathematics of infectious diseases, SIAM Rev. **42**, 599 (2000).

[5] R. M. Anderson and R. M. May, *Infectious Diseases of Humans: Dynamics and Control* (Oxford University Press, Oxford, 1991).

[6] H. Salje, C. Tran Kiem, N. Lefrancq, N. Courtejoie, P. Bosetti, J. Paireau, A. Andronico, N. Hozé, J. Richet, C.-L. Dubost,

Estimating the burden of SARS-CoV-2 in France, Science **369**, 208 (2020).

[7] N. T. Bailey, *The Mathematical Theory of Infectious Diseases and its Applications* (Charles Griffin & Company Ltd, 5a Crendon Street, High Wycombe, Bucks HP13 6LE, 1975).

[8] D. G. Kendall, Deterministic and stochastic epidemics in closed populations, in *Proceedings of the Third Berkeley Symposium on Mathematical Statistics and Probability* (University of California Press, Berkeley, 1956), Vol. 4, pp. 149–165.

[9] T. Harko, F. S. Lobo, and M. Mak, Exact analytical solutions of the susceptible-infected-recovered (SIR) epidemic model and of the SIR model with equal death and birth rates, Appl. Math. Comput. **236**, 184 (2014).

[10] D. Prodanov, Analytical solutions and parameter estimation of the SIR epidemic model, Mathematical Analysis of Infectious Diseases 163 (2022).

[11] A. M. Carvalho and S. Gonçalves, An analytical solution for the Kermack–McKendrick model, Physica A **566**, 125659 (2021).

[12] H. Li and S. Guo, Dynamics of a SIRC epidemiological model, Electr. J. Differ. Equ. **2017**, 1 (2017).

[13] M. Y. Li, H. L. Smith, and L. Wang, Global dynamics of an SEIR epidemic model with vertical transmission, SIAM J. Appl. Math. **62**, 58 (2001).

[14] D. Sen and D. Sen, Use of a modified SIRD model to analyze Covid-19 data, Ind. Eng. Chem. Res. **60**, 4251 (2021).

[15] S. Gao, Z. Teng, J. J. Nieto, A. Torres, Analysis of an SIR epidemic model with pulse vaccination and distributed time delay, J. Biomed. Biotechnol. **2007**, 64870 (2007).

[16] G. Kozyreff, Asymptotic solutions of the SIR and SEIR models well above the epidemic threshold, IMA J. Appl. Math. **87**, 521 (2022).

[17] L. Fumanelli, M. Ajelli, P. Manfredi, A. Vespignani, and S. Merler, Inferring the structure of social contacts from demographic data in the analysis of infectious diseases spread, PLoS Comput. Biol. **8**, e1002673 (2012).

[18] D. Mistry, M. Litvinova, A. Pastore y Piontti, M. Chinazzi, L. Fumanelli, M. F. Gomes, S. A. Haque, Q.-H. Liu, K. Mu, X. Xiong, Inferring high-resolution human mixing patterns for disease modeling, Nat. Commun. **12**, 323 (2021).

[19] N. Ferguson, D. Laydon, G. Nedjati Gilani, N. Imai, K. Ainslie, M. Baguelin, S. Bhatia, A. Boonyasiri, Z. Cucunuba, G. Cuomo-Dannenburg *et al.*, Report 9: Impact of non-pharmaceutical interventions (NPIs) to reduce Covid-19 mortality and healthcare demand, Imperial College London COVID-19 (2020).

[20] L. Bremaud and D. Ullmo, Social structure description of epidemic propagation with a mean-field game paradigm, Phys. Rev. E **106**, L062301 (2022).

[21] D. J. Watts and S. H. Strogatz, Collective dynamics of 'small-world'networks, Nature (London) **393**, 440 (1998).

[22] F. C. Santos, J. F. Rodrigues, and J. M. Pacheco, Epidemic spreading and cooperation dynamics on homogeneous small-world networks, Phys. Rev. E **72**, 056128 (2005).

[23] D. H. Silva, F. A. Rodrigues, and S. C. Ferreira, High prevalence regimes in the pair-quenched mean-field theory for the susceptible-infected-susceptible model on networks, Phys. Rev. E **102**, 012313 (2020).

[24] S. Mizutaka, K. Mori, and T. Hasegawa, Synergistic epidemic spreading in correlated networks, Phys. Rev. E **106**, 034305 (2022).

[25] M. Barthélemy, A. Barrat, R. Pastor-Satorras, and A. Vespignani, Dynamical patterns of epidemic outbreaks in complex heterogeneous networks, J. Theor. Biol. **235**, 275 (2005).

[26] Y. Hu, L. Min, and Y. Kuang, Modeling the dynamics of epidemic spreading on homogenous and heterogeneous networks, Applicable Analysis **94**, 2308 (2015).

[27] F. D. Sahneh and C. Scoglio, Epidemic spread in human networks, in *2011 50th IEEE Conference on Decision and Control and European Control Conference* (IEEE, Orlando, FL, USA, 2011), pp. 3008–3013.

[28] M. E. Newman, Spread of epidemic disease on networks, Phys. Rev. E **66**, 016128 (2002).

[29] L. Di Domenico, Data-driven modeling of COVID-19 spread in France to inform pandemic response, Ph.D. thesis, Sorbonne Université, 2022.

[30] R. Pastor-Satorras, C. Castellano, P. Van Mieghem, and A. Vespignani, Epidemic processes in complex networks, Rev. Mod. Phys. **87**, 925 (2015).

[31] W. Wang, M. Tang, H. E. Stanley, and L. A. Braunstein, Unification of theoretical approaches for epidemic spreading on complex networks, Rep. Prog. Phys. **80**, 036603 (2017).

[32] Web of science citation report for the query "epidemic on networks", https://www-webofscience-com.inp.bib.cnrs.fr/wos/woscc/citation-report/e9511ae6-cc49-4efe-bd8d-41fc80a2ab17-caa9b524 (2024).

[33] L. J. Allen, An introduction to stochastic epidemic models, *Mathematical Epidemiology* (Springer, 2008), pp. 81–130.

[34] P. L. Simon and I. Z. Kiss, Super compact pairwise model for SIS epidemic on heterogeneous networks, J. Complex Netw. **4**, 187 (2016).

[35] M. J. Keeling, The effects of local spatial structure on epidemiological invasions, Proc. R. Soc. London B **266**, 859 (1999).

[36] N. C. Wormald, The asymptotic connectivity of labelled regular graphs, J. Comb. Theory, Ser. B **31**, 156 (1981).

[37] S. N. Dorogovtsev, A. V. Goltsev, J. F. Mendes, and A. N. Samukhin, Spectra of complex networks, Phys. Rev. E **68**, 046109 (2003).

[38] F. Goirand, B. Georgeot, O. Giraud, and S. Lorthois, Network community structure and resilience to localized damage: Application to brain microcirculation, Brain Multiphysics **2**, 100028 (2021).

[39] I. Z. Kiss, E. Kenah, and G. A. Rempała, Necessary and sufficient conditions for exact closures of epidemic equations on configuration model networks, J. Math. Biol. **87**, 36 (2023).

[40] J. H. Lambert, Observationes variae in mathesin puram, Acta Helvetica **3**, 128 (1758).

[41] R. M. Corless, G. H. Gonnet, D. E. Hare, D. J. Jeffrey, and D. E. Knuth, On the Lambert W function, Adv. Comput. Math. **5**, 329 (1996).

[42] L. Euler, De serie Lambertina plurimisque eius insignibus proprietatibus, Acta Academiae scientiarum imperialis petropolitanae 29 (1783).

[43] D. Belkić, All the trinomial roots, their powers and logarithms from the Lambert series, Bell polynomials and Fox-Wright function: Illustration for genome multiplicity in survival of irradiated cells, J. Math. Chem. **57**, 59 (2019).

[44] M. Glasser, Hypergeometric functions and the trinomial equation, J. Comput. Appl. Math. **118**, 169 (2000).

[45] A.-L. Barabási and R. Albert, Emergence of scaling in random networks, Science **286**, 509 (1999).